HHS Public Access

Author manuscript

Anal Methods. Author manuscript; available in PMC 2021 April 21.

Published in final edited form as:

Anal Methods. 2020 April 21; 12(15): 2046–2051. doi:10.1039/d0ay00368a.

3D-Printed Microfluidic Device with In-line Amperometric Detection that Also Enables Multi-Modal Detection

Elizabeth A. Hayter, **Andre D. Castiaux**, **R. Scott Martin***

Department of Chemistry, Saint Louis University

Abstract

Microfluidic amperometric detectors often include a reservoir to house auxiliary and reference electrodes, making subsequent detection downstream challenging. Here, we present an in-line microfluidic device with amperometric detection that incorporates a three-electrode set-up, made possible by threading electrodes into a 3D-printed flow cell. The electrodes consist of a commercially available threaded reference electrode and electrodes fabricated in commercially available fittings. This approach centers the working electrode in the fluidic channel enabling the use of a pillar working electrode that is shown to increase sensitivity, as compared to a traditional thin-layer electrode. In addition, the working and auxiliary electrodes can be directly opposed, with this configuration leading to a more uniform potential being applied to the working electrode as well as fewer issues with any iR drop. To demonstrate the ability to incorporate a separate mode of detection downstream from the electrochemical flow cell, the device is modified to include a mixing T for introduction of reagents for chemiluminescent detection of ATP (via the luciferin-luciferase reaction), leading to a single 3D-printed device that can be used to detect norepinephrine and ATP, nearly simultaneously, by amperometry and chemiluminescence, respectively. This approach opens numerous possibilities, where microfluidics with in-line amperometry can be used in continuous circulation studies or in conjunction with other downstream detection events to study complex systems.

Introduction

Use of 3D-printing to create microfluidic devices has recently emerged as a leading alternative over use of standard fabrication methods. With small channels (100's of μm or less) and small reagent volumes, microfluidics provides a sensitive analytical approach to complete tasks in a faster and more inexpensive fashion. The ability to incorporate flow to induce shear stress has advanced cell-culture research as the microenvironment better mimics the *in vivo* environment. Analytes, such as cell contents or releasates, undergo minimal dilution and can be analyzed with high temporal resolution.[1] Application of 3D-printing to microfluidics brought new design possibilities that were previously unattainable with the traditional fabrication materials of silicon, glass, and PDMS, for example, threads and inserts can be incorporated into devices.[2,3] 3D-prints are reusable and versatile compared to the more traditional microfluidic counterparts. They are simple to fabricate and

*corresponding author: Dr. R. Scott Martin, 3501 Laclede Ave, St. Louis, MO, USA 63103, +1 314-977-2836, scott.martin@slu.edu.

obviate the need for expensive microfluidic fabrication facilities. Files can be easily shared and modified, aiding in collaborations and reproducibility across labs.

Microfluidic-based amperometric flow cells, which have been fabricated historically with sputtering and lithography,[4-6] have also benefitted from 3D-printing. The first incorporation of electrochemical detection in 3D-printed fluidic devices by Erkal et al. described a threaded device for electrodes fabricated in commercially available PEEK fittings.[7] The design provided flexibility of electrode material and ease of electrode replacement after fouling or electrode polishing. There were some issues with this design, however. The thin-layer design housed both the working and pseudo-reference electrodes in a single fitting. This resulted in the two electrodes needing to be aligned in the channel while being threaded far enough to seal the channel. An opportunity for 3D printing is to address the fact that most microfluidic amperometric detection devices lack the ability to incorporate the associated electrodes, auxiliary and reference, in the flow stream as commonly seen in HPLC flow cells.[8] For microchip devices, it is common to place these electrodes in a fluidically connected chamber such as a reservoir.[9,10] Disadvantages of this approach include the manual nature with which these are placed in the reservoir as well as the inability for any downstream processes after electrochemical detection, as the analyte is greatly diluted in the reservoir. For situations where multi-modal detection is desired, researchers are left with the options of splitting the flow or having electrochemistry as the final detection method. Another option is the use of a two-electrode system, with a pseudo-reference. While this has been accomplished with screen printed electrodes or embedded electrodes,[11,12] the measured potential can be less accurate due to the lack of thermodynamic equilibrium.[13] Many labs have turned to fabricating their own reference electrode for their system.[14,15] The Boutelle lab has created thread-type inserts containing a self-made reference electrode and working electrode in a needle tip.[16,17] Whether the electrode is a pseudo-reference or a true reference, the problem still stands of how to incorporate the electrode into a channel.

Here, we present a 3D-printed microfluidic device to address these issues, with in-line amperometric detection using a three-electrode set-up and threaded electrodes including a commercially available threaded reference electrode. The working/auxiliary electrode configuration used here is referred to as a parallel-opposed electrode configuration in which two electrodes are directly across the channel from each other.[8,18] The Schoenfisch lab has lithographically produced an amperometric detection chip of this design with planar electrodes.[19] The approach described here can easily be assembled and disassembled while keeping all of the detection electrodes in the fluidic network without the use of a reservoir. A key feature of the device is that other detection modes can be placed downstream since a reservoir is avoided. We show the in-line capability of the approach by modifying the device to include downstream detection of ATP via the luciferin-luciferase assay. In this, we have created a single 3D-printed microfluidic device that can be used to nearly simultaneously detect norepinephrine and ATP using two different modes of detection—amperometry and chemiluminescence.

Materials and Methods

3D-Printed device design and fabrication

Microfluidic devices were designed in Autodesk Inventor Professional and printed on an ObJet Eden 260 V 3D Printer (Stratasys, Edin Prairie, MN, USA) using proprietary, acrylate-based Full Cure 720 (Stratasys, Edin Prairie, MN, USA) model material.[20] All voids were filled with Full Cure 705 (Stratasys, Edin Prairie, MN, USA) support material. The support material was removed mechanically and via sonication with a final rinse with isopropanol and water. The 3D-printed devices were wet polished with 800-1200 grit polishing pads to achieve optical clarity.

The amperometric device (Figure 1) consists of a 500 x 500 μm channel with threads designed to fit commercial fittings for flow input and output (Idex Health & Science, Oak Harbor, WA P-202X) as well as for the fabricated or commercially available electrodes (Idex Health & Science, Oak Harbor, WA P-235). The device was designed with open channels where the electrodes are placed so that the electrodes are threaded in to seal the channel and form the channel wall. The working and auxiliary electrodes thread into the device from opposite sides resulting in face-to-face electrode surfaces on two opposite walls of the channel. A channel support the width of the channel acts as a stop for the electrodes and maintains channel shape (Figures 1B and 2A). Although the resolution of the printer permits lower, the channel size of this device was limited to a minimum of 500 x 500 μm to be reliably cleaned of support material and to maintain structural stability to stop the electrodes at channel contact. Larger channel sizes decreased the sensitivity of the device. A CH Instruments screw type Ag/AgCl reference electrode was used as the reference (RE-3VT, CH Instruments, Austin, TX). The insertion point was designed to fit the electrode such that the channel is sealed and there is no dead volume. Complete CAD drawings (Figures S1 and S2) and .stl files can be found in the Supplementary Information.

Electrode fabrication

Fabrication of electrodes embedded in fittings has been previously reported.[7,20] The electrode material of choice was attached to copper wire with colloidal silver paste and insulated with heat shrink tubing. The wire was placed into a fitting (Idex Health & Science, Oak Harbor, WA) and held in position with 5-minute epoxy (Permatex, Solon, OH) on the backside of the fitting. The electrode wire was centered and a mixture of 12:1 m/m ratio of Armstrong C-7 Adhesive and Armstrong Activator A (Ellsworth Adhesives, Germantown, WI) was applied into the threaded end of the fitting and cured at room temperature overnight. The electrodes were polished smooth using 800-1200 grit polishing pads (Buehler, Lake Bluff, IL). To enhance sensitivity, a three-dimensional gold pillar was deposited on gold working electrodes through electrodeposition (Figure 2A).[7,21] A 100 μm flat gold electrode (Alfa Aesar, Haverhill, MA), a platinum wire auxiliary electrode (Alfa Aesar, Haverhill, MA), and a Ag/AgCl reference electrode (CH instruments, Austin, TX) were placed in a solution of 50 mM dicyanoaurate(I) (Sigma-Aldrich, St Louis, MO) in 0.1 M Na_2CO_3 (Sigma-Aldrich, St. Louis, MO) and a potential of −1.2 V (vs. Ag/AgCl) was applied to the gold electrode. Pillar height is proportional to deposition time and was

measured using a profilometer (Dektak[3]ST, Veeco Instruments, Plainview, NY) and imaged using a stereoscope (Olympus SZ61, Olympus Life Science, Tokyo, Japan).[7]

Amperometry Studies

For device assembly, a freshly polished 100 μm gold working electrode was threaded into place, sealed against the channel support, and confirmed that the electrode was indeed centered in the channel before the 500 μm platinum auxiliary electrode was threaded into place (Figure 2A). A CH Instruments Ag/AgCl reference electrode was threaded into place to seal the channel and maintain contact with the flow channel. The working and auxiliary electrodes were separated by the width of the channel (500 μm) and the reference electrode was approximately 10 mm downstream. The flow was controlled by a syringe pump (Harvard Apparatus, Holliston, MA) and injections were made using a 4-port rotary injection value (Valco Instruments, Houston, TX). The syringe was connected to the 4-port using Tygon tubing (Cole Parmer, Vernon Hills, IL) with fingertight PEEK fittings (Idex Health & Science, Oak Harbor, WA) and a luer-lock adaptor (Idex Health & Science, Oak Harbor, WA). A 150 μm capillary (Polymicro Technologies, Phoenix, AZ) was used to connect the 4-port injector to the device with 400 μm i.d. nanotight sleeves adapters (Idex Health & Science, Oak Harbor, WA). For all studies, PBS (Sigma-Aldrich, St Louis, MO) as pumped at 15 μL/min from a 1 mL glass, air-tight syringe (Scientific Glass Engineering, Melbourne, Australia, and Hamilton Company, Reno, NV) and injections were made using a 500 nL rotor. A CH Instruments 812B potentiostat applied a potential of +0.9 V (vs. Ag/AgCl) to the working electrode for detection. Characterization of the device was conducted using standards of catechol (Sigma-Aldrich, St Louis, MO) in PBS. All solutions were prepared the day of use. For LOD calculations, amperograms were smoothed with a fifteen point least square smooth (using CH Instruments software) to filter out noise.

Voltammetry Study

The electrochemical effects of the auxiliary electrode position were examined via linear sweep voltammetry. The electrode configuration consisted of the auxiliary electrode placed either directly opposite the working electrode or, similar to past work, in a downstream reservoir.[20,21] The device was modified to contain a reservoir at the end of the channel (Figure 3A). For the opposed configuration, all electrodes were assembled as designed. No pillar was deposited on the working electrode for this comparison. To examine the effects of placing the auxiliary electrode in the reservoir (instead of opposite the working electrode), the auxiliary electrode connection was made to a 500 μm diameter platinum auxiliary electrode (in a fitting) placed in the reservoir. Linear sweep voltammograms were taken of 10 mM ferricyanide (Sigma-Aldrich, St Louis, MO) in 0.5 M KCl (Fisher Scientific, Fair Lawn, NJ) at a flow rate of 15 μL/min (Figure 3B). The potential was scanned from +0.7 to −0.3 V (vs. Ag/AgCl) at a scan rate of 0.01 V/s. Data shown in Figure 3 is the result of averaging three scans.

Multi-modal characterization

To show the possibility of subsequent downstream detection (post-amperometry), the device design was altered to include a separate port for reagent addition and a channel for mixing and chemiluminescent detection of ATP (Figure 4A-B). A second input for reagent was

added at a 90° angle to the channel and the output channel extended to form a mixing T and a reaction and detection channel. ATP detection occurred via the luciferin-luciferase assay as previously reported.[22] For this assay, 50 mg of crude firefly lanterns (Sigma-Aldrich, St Louis, MO) and 3.2 mg of D-luciferin (Gold Biotechnology, St. Louis, MO) were dissolved in 10 mL of PBS and sterile-filtered. A syringe pump was used to continuously pump reagent through the device at 15 μL/min. The multi-modal device was placed on top of a PMT (Hamamatsu Photonics, Shizuoka, Japan) in a light-excluding box.[22] Voltage from the PMT was monitored for ATP quantification. ATP (Sigma-Aldrich, St Louis, MO) and norepinephrine (Sigma-Aldrich, St Louis, MO) standards were made in PBS the day of use. Traces shown in Figure 4C were smoothed in PeakFit (San Jose, CA) with a small Savitzky-Golay filter (0.5% window) for presentation purposes (to help filter noise).

Results and Discussion

Figure 1 shows the 3D-printed amperometric flow cell that was developed. The device incorporates a three-electrode system, using a commercially available threaded reference electrode in channel and an auxiliary electrode that is threaded directly opposite the working electrode (instead of placing such electrodes in a reservoir). This allows subsequent detection downstream without significant dilution. This device uses the threaded electrodes to seal the channel by acting as the channel wall. A channel support acts as an electrode stop so that the flow is not disrupted or blocked by the electrode fitting. It is also used to maintain channel shape. The channel support is the thickness of the channel (500 μm). When the channel support was not included in the print, the sensitivity of the device suffered due to the large dead volume (this was an issue in our earlier report[7]). In addition to increasing the limit of detection, the dilution of the plugs of analyte would be disadvantageous for downstream detection. Confocal images of the electrode forming the channel wall against the channel support can be found in Figure S3. The 3D-printed device is robust enough to withstand insertion and removal of electrodes for polishing and cleaning as desired and devices have been used for days to weeks on end.

One advantage that this design has over our previous 3D-printed in-line amperometric flow cell[7] is that there is a single electrode centered in the middle of each fitting. This makes assembly very simple and produces a device that is compatible with external deposition of a gold pillar on the working electrode to enhance sensitivity. Despite the rotation of threading the fitting in to seal the channel, the electrode is always centered in the channel. While most electrodes are of the thin-layer variety, we wanted to explore the use of a pillar on the working electrode to increase the electrode surface area and, more importantly, protrude into the channel to increase mass transfer of analyte to the electrode (see Figure 2A and S3). Increasing the pillar height significantly increases the sensitivity of the device (Figure 2B). As can be seen with the calibration curves, compared to a flat electrode, a 30 μm pillar increases the sensitivity by three times, and a 95 μm pillar increases it by over eight times. For a flat gold electrode, the limit of detection was 620 nM, and the use of an 80 μm pillar improved the limit of detection to 340 nM.

The change in electrode configuration has two ramifications apart from making in-line detection possible. The first is based on the orientation of the working and auxiliary

electrodes, as described previously for LC and CE flow cell design.[23] When the auxiliary electrode is directly opposite the working, the current flow is perpendicular to the planar electrode and the working electrode has a more uniform potential across its surface. Second, as shown with the linear sweep voltammograms of ferricyanide in Figure 3B, the half-wave potential of the reservoir configuration is shifted toward higher potentials, as compared to the parallel-opposed configuration. As described in a comprehensive review of the subject for LC-EC,[23] a reservoir configuration for the auxiliary electrode can lead to iR drop issues due to significant solution resistance, resulting in a lower potential at the working electrode. With the parallel-opposed configuration, the current flows between the working and auxiliary, directly across the channel, with little to no iR drop from solution resistance. The data in Figure 3 shows that for a three-electrode system in microfluidic devices, a parallel-opposed configuration has distinct advantages.

In addition to the improved performance of this approach, to demonstrate the opportunities afforded by these in-line capabilities the device design was modified to include a flow port for the addition of luciferin-luciferase reagent that is mixed with the flow in a reaction channel for the detection of ATP after the electrochemical portion of the device (Figure 4A-B). In doing so, we created a device that can be used to nearly simultaneously detect norepinephrine and ATP via two different detection modes—amperometry and chemiluminescence—on a single 3D-printed device. Norepinephrine and ATP are two transmitters co-released by sympathetic nerves and are of interest to hypertension pathophysiology.[24,25] These small molecules are often quantified through HPLC and derivatization detection schemes, but the offline nature causes dilution and leaves time for oxidation. The microfluidic approach published by Townsend et al. used a droplet splitter, amperometric detection chip, mixing T, and luminometer to analyze norepinephrine and ATP from perfusate of the mesenteric arterial bed of a rat in close-to-real time.[26] Here we show that the scheme can be pared down to a single device. Norepinephrine is detected amperometrically using a 100 μm gold (flat) electrode and ATP is detected through the highly specific chemiluminescent reaction with the luciferase enzyme in the presence of luciferin.[27,28] To achieve optical clarity, the device was wet polished and placed atop a PMT in a light-excluding box. Plugs of the analytes, norepinephrine and ATP in PBS, were injected onto the device and peak area for each was measured. The chemiluminescent signal peaked 15 seconds after the amperometric signal, which agrees with the time delay calculation based on the distance between the two detection schemes, the shape of the channel, the flow rate, and ATP/luciferin-luciferase reaction time, which is nearly instantaneous.[29] Multi-modal traces can be seen in Figure 4C. No interference was seen between detection modes as shown in Figure 4C in which large concentrations of analyte (200 μM norepinephrine and 500 μM ATP) were injected onto the device. In addition, no statistical difference in signal was seen between injections of ATP alone and injections of ATP with the addition of NE (and vice versa, calibration curves shown in Figure S4). Each detection method is, therefore, selective to its intended analyte. The limit of detection for norepinephrine was 600 nM and for ATP was 840 nM. It is clear that this type of device can be used to selectively detect two different analytes by two different detection modes. Having the electrochemical detection scheme prior to any reaction or derivatization portion of the

device ensures that the electrochemically active analyte is not diluted or subject to any of the reaction chemistry if the second detection mode requires a derivatization/reaction.

Conclusion

In this paper we have introduced a 3D-printed, three-electrode system amperometric flow cell that incorporates an in-line reference electrode and an opposed auxiliary electrode, without the need for a reservoir. Three electrodes are threaded into the device to seal the channels with the working electrode placed directly opposite the auxiliary electrode, a design that is very difficult with traditional microfluidic fabrication methods. This orientation change leads to a more uniform potential being applied to the working electrode as well as fewer issues with any iR drop. This design change is easy to assemble and is compatible with electrodeposition of a gold pillar on the working electrode to increase sensitivity. We have also shown the in-line capabilities of the device by printing a multi-modal device that can be used to detect norepinephrine and ATP via amperometry and chemiluminescence, nearly simultaneously. Going forward, we plan further to optimize the device to enable in-line amperometric detection of challenging analytes such as nitric oxide so that ATP-derived vasodilation mechanisms can be studied. The modular nature of the device pairs well with the previously published 3D-printed cell-culture module and inserts.[30,31] In addition, because of the lack of reservoir, the in-line amperometric device can be used in circulation studies. With easily exchanged and modifiable electrodes, this device can be used to detect any electrochemically active analyte.

Supplementary Material

Refer to Web version on PubMed Central for supplementary material.

Acknowledgements

Support from the National Institutes of Health (NS105888) is acknowledged. The authors would also like to thank Prof. Istvan Kiss from Saint Louis University for helpful discussions.

References

1. Castiaux AD, Spence DM and Martin RS, Anal Methods, 2019, 11, 4220. [PubMed: 32051693]
2. Gross BC, Erkal JL, Lockwood SY, Chen C and Spence DM, Anal Chem, 2014, 86, 3240. [PubMed: 24432804]
3. Chen C, Mehl BT, Munshi AS, Townsend AD, Spence DM and Martin RS, Anal Methods, 2016, 8, 6005. [PubMed: 27617038]
4. Martin RS, in Methods in Molecular Biology, ed. Henry CS, Humana Press, Totowa, NJ, 2006, vol. 339.
5. Batz NG and Martin RS, Analyst, 2009, 134, 372. [PubMed: 19173065]
6. Scott DE, Grigsby RJ and Lunte SM, Chemphyschem, 2013, 14, 2288. [PubMed: 23794474]
7. Erkal JL, Selimovic A, Gross BC, Lockwood SY, Walton EL, McNamara S, Martin RS and Spence DM, Lab Chip, 2014, 14, 2023. [PubMed: 24763966]
8. Roston DA, Shoup RE and Kissinger PT, Anal Chem, 1982, 54, 1417A.
9. Martin RS, Gawron AJ and Lunte SM, Anal Chem, 2000, 72, 3196. [PubMed: 10939387]
10. Vickers JA, Caulum MM and Henry CS, Anal Chem, 2006, 78, 7446. [PubMed: 17073411]

11. de Oliveira RAG, Materon EM, Melendez ME, Carvalho AL and Faria RC, ACS Appl Mater Interfaces, 2017, 9, 27433. [PubMed: 28742317]
12. Agustini D, Bergamini MF and Marcolino-Junior LH, Lab Chip, 2016, 16, 345. [PubMed: 26659997]
13. Inzelt G, in Handbook of Reference Electrodes, eds. Inzelt G, Lewenstam A and Scholz F, Springer, Berlin, Heidelberg, 2013, pp. 331.
14. Zhou J, Ren K, Zheng Y, Su J, Zhao Y, Ryan D and Wu H, Electrophoresis, 2010, 31, 3083. [PubMed: 20803753]
15. Zhang H, Chuai R, Li X and Zhang B, Micromachines, 2018, 9, 114.
16. Gowers SAN, Curto VF, Seneci CA, Wang C, Anastasova S, Vadgama P, Yang G and Boutelle MG, Anal Chem, 2015, 87, 7763. [PubMed: 26070023]
17. Samper IC, Gowers SAN, Rodgers ML, Murray DRK, Jewell SL, Pahl C, Strong AJ and Boutelle MG, Lab Chip, 2019, 19, 2038. [PubMed: 31094398]
18. Roston DA and Kissinger PT, Anal Chem, 1982, 54, 429.
19. Hunter RA and Schoenfisch MH, Anal Chem, 2015, 87, 3171. [PubMed: 25714120]
20. Munshi AS and Martin RS, Analyst, 2016, 141, 862. [PubMed: 26649363]
21. Townsend AD, Sprague RS and Martin RS, Electroanalysis, 2019, 31, 1409.
22. Castiaux AD, Pinger CW, Hayter EA, Bunn ME, Martin RS and Spence DM, Anal Chem, 2019, 91, 6910. [PubMed: 31035747]
23. Lunte SM, Lunte CE and Kissinger PT, in Laboratory Techniques in Electroanalytical Chemistry, Revised and Expanded, eds. Kissinger PT and Heineman WR, Marcel Dekker, Inc., New York, NY, 2 edn., 1996.
24. Sperlagh B, Sershen H, Lajtha A and Vizi ES, Neuroscience, 1998, 82, 511. [PubMed: 9466457]
25. Wier WG, Zang W, Lamont C and Raina H, Exp Physiol, 2009, 94, 31. [PubMed: 18931047]
26. Townsend AD, Wilken GH, Mitchell KK, Martin RS and Macarthur H, J Neurosci Methods, 2016, 266, 68. [PubMed: 27015793]
27. Hammerstedt RH, Anal Biochem, 1973, 52, 449. [PubMed: 4698838]
28. Spielmann H, Jacob-Mueller U and Schulz P, Anal Biochem, 1981, 113, 172. [PubMed: 7270882]
29. Marques SM and Esteves da Silva JC, IUBMB Life, 2009, 61, 6. [PubMed: 18949818]
30. Chen C, Townsend AD, Hayter EA, Birk HM, Sell SA and Martin RS, Anal Bioanal Chem, 2018, 410, 3025. [PubMed: 29536154]
31. Mehl BT and Martin RS, Anal Methods, 2019, 11, 1064. [PubMed: 31244918]

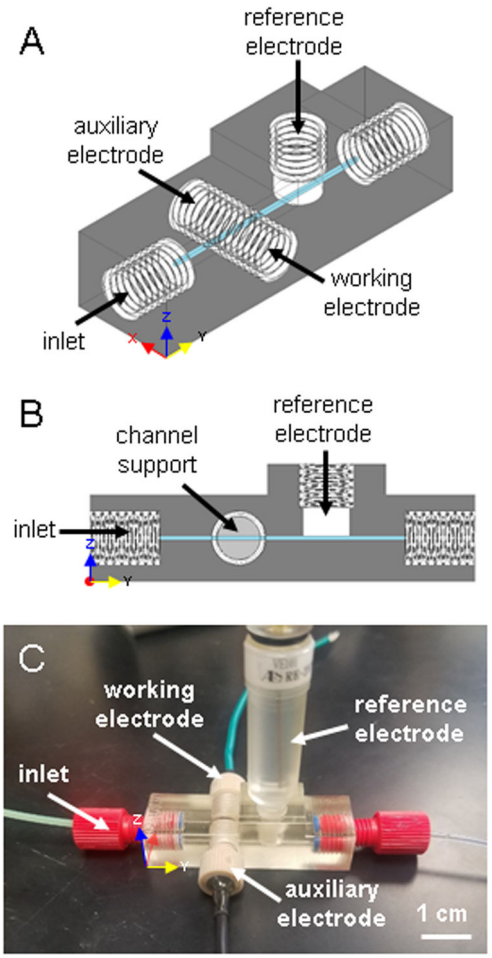

Figure 1.

3D-printed, in-line amperometric detection device. (A) CAD rendering of the device. (B) Side view of the device highlighting the channel support, which acts as an electrode stop and maintains consistent channel shape. (C) Photograph of the device. Assembled, it houses the fabricated working and auxiliary electrodes, and a commercially available Ag/AgCl reference electrode (already threaded), and two fittings for flow input and output.

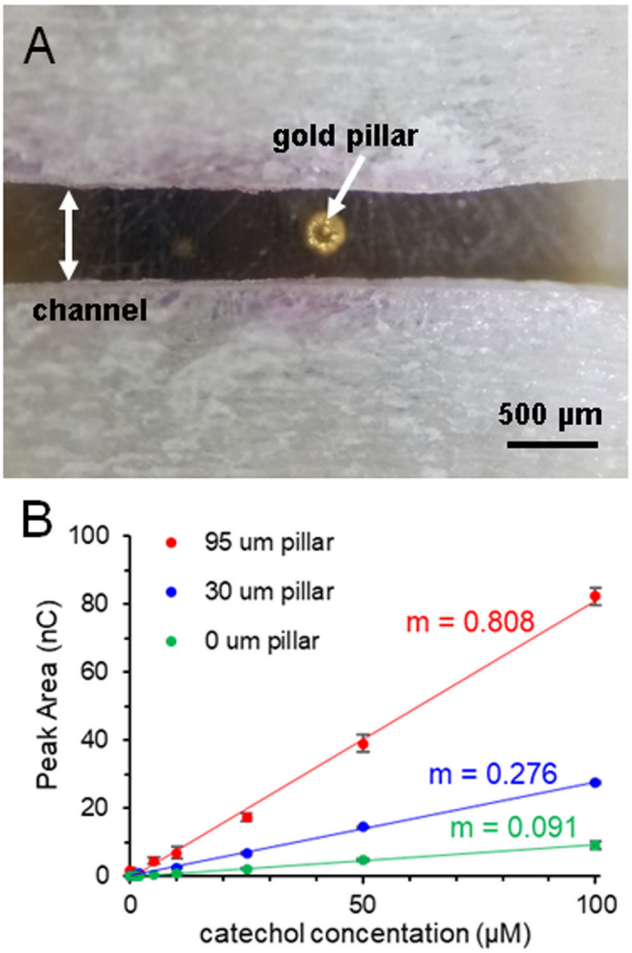

Figure 2.

Use of gold pillar for signal enhancement. (A) Micrograph of gold pillar deposited on a 100 µm gold working electrode, centered in the channel (pillar height = 70 µm). (B) Effect of pillar height on calibration sensitivity (expressed as the slope, m), with larger pillar heights leading to significant increases (500 nL injections of catechol in PBS, $r^2 \geq 0.997$). Error bars signify standard deviation ($n \geq 3$).

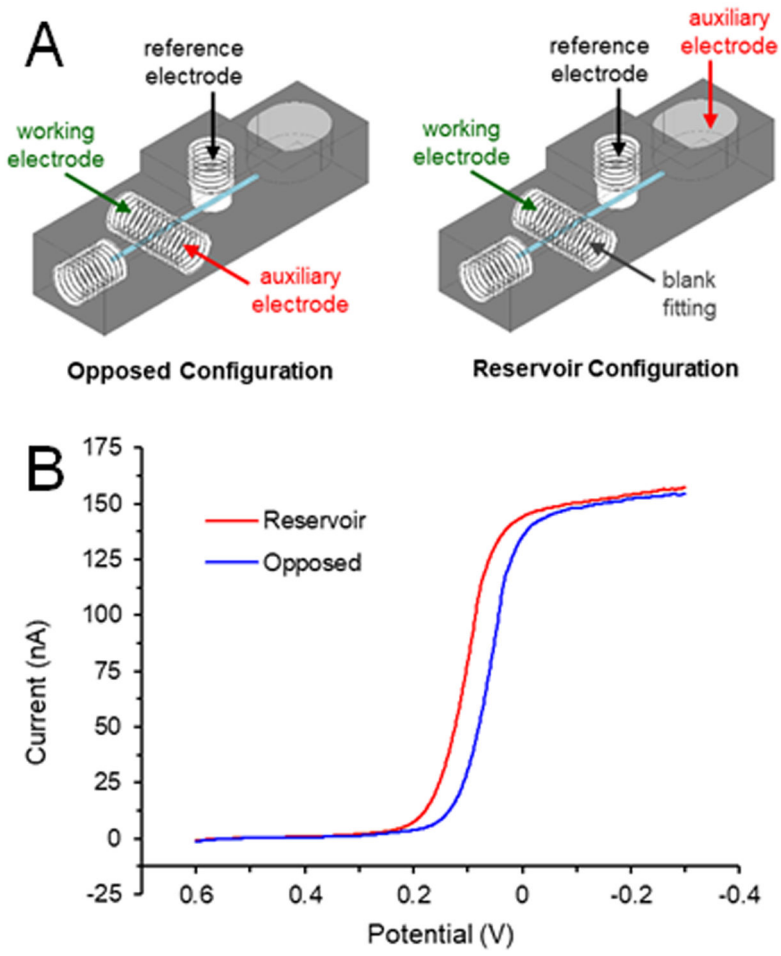

Figure 3.

Effects of electrode orientation on voltammogram. (A) Diagrams of the electrode placements. The auxiliary electrode was placed either opposite the working electrode (blue trace in B) or downstream in the reservoir (red trace in B). (B) Linear sweep voltammograms of 10 mM ferricyanide (in 0.5 M KCl) under flowing conditions (pumping solution at 15 μL/min).

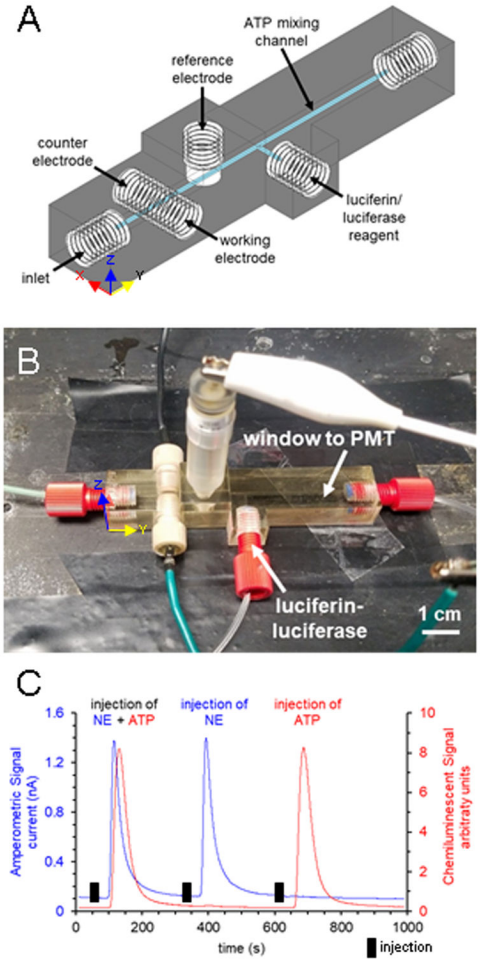

Figure 4.

3D-printed multi-modal device featuring amperometric detection for norepinephrine and downstream chemiluminescent detection for ATP. (A) CAD rendering of the device. (B) Photograph of assembled device with sample inlet, three detection electrodes, an inlet for the luciferin-luciferase reagent, and output to waste. The ATP mixing channel denoted in (A) is placed over a PMT. (C) Flow injection analysis of injections of 500 μM norepinephrine and 200 μM ATP, 500 μM norepinephrine alone, and 200 μM ATP alone.